Appl. Sci. **2014**, *4*, 468-481; doi:10.3390/app4030468

OPEN ACCESS

applied sciences

ISSN 2076-3417

www.mdpi.com/journal/applsci

Article

Effect of RhOx/CeO_2 Calcination on Metal-Support Interaction and Catalytic Activity for N_2O Decomposition

Verónica Rico-Pérez † and Agustin Bueno-López †,*

Department of Inorganic Chemistry, University of Alicante, Ap.99, E-03080 Alicante, Spain;
E-Mail: veronica.rico@ua.es

† These authors contributed equally to this work.

* Author to whom correspondence should be addressed; E-Mail: agus@ua.es;
Tel.: +34-600-948-665; Fax: +34-965-903-454.

Received: 22 August 2014; in revised form: 10 September 2014 / Accepted: 10 September 2014 / Published: 22 September 2014

Abstract: The effect of the calcination conditions on the catalytic activity for N_2O decomposition of 2.5% RhOx/CeO_2 catalysts has been investigated. Ramp and flash calcinations have been studied (starting calcinations at 25 or 250/350 °C, respectively) both for cerium nitrate and ceria-impregnated rhodium nitrate decomposition. The cerium nitrate calcination ramp has neither an effect on the physico-chemical properties of ceria, observed by XRD, Raman spectroscopy and N_2 adsorption, nor an effect on the catalysts performance for N_2O decomposition. On the contrary, flash calcination of rhodium nitrate improved the catalytic activity for N_2O decomposition. This is attributed to the smaller size of RhOx nanoparticles obtained (smaller than 1 nm) which allow a higher rhodium oxide-ceria interface, favoring the reducibility of the ceria surface and stabilizing the RhOx species under reaction conditions.

Keywords: N_2O decomposition; Rh; ceria; Rh-ceria interaction; nanoparticles; subnanoparticles; nitric acid plant; ceria catalyst

---

1. Introduction

Cerium dioxide powders have potential applications in polishing powders, coatings for high-temperature optical and ceramic materials, gas sensors, catalysts for environmental processes like Three Way Catalyst (TWC), wet catalytic oxidation of organic pollutants (removal of organics from wastewaters), water gas shift (WGS) reaction, CO oxidation, combustion processes or in solid oxide fuel cell technology [1,2]. The interest of ceria-based materials is related to their structural and chemical properties, low temperature reducibility, oxygen storage capacity, and oxygen release properties among others.

In catalytic applications, ceria is used either as metal support or as catalyst itself [1,3]. The use of ceria as noble metal support has attracted intense interest due to their vast applications in heterogeneous catalysis. Many factors, including the size and distribution of the noble metal particles, the surface morphology and defects on the oxides, affect the performance of noble metal/ceria catalysts. Indeed, effectively controlling the size of noble metal particles is crucial for maintaining high catalytic activity. The behavior of the metal-oxide interface, which can be quite dynamic, as exemplified by the well-known strong metal-support interaction (SMSI), is of critical importance in this regard [1–5].

The promoting effect of CeO_2-based materials in the catalytic activity of rhodium, and other platinum group metals (PGM), is very well known for several chemical reactions [3–16], like in three-way catalysts (TWC) where NOx, hydrocarbons and CO are simultaneously depleted [16].

N_2O decomposition on ceria-supported noble metal catalysts was investigated in a previous work, where noble metals (Rh, Pd and Pt) were supported on γ-Al_2O_3, pure CeO_2 and La- and Pr-doped CeO_2 [17]. Rh was the best noble metal, and the support strongly affected the activity, ceria-based supports being better as rhodium support than alumina. In a further study [18], the $Rh/Ce_{0.9}Pr_{0.1}O_2$ active phase was supported on a cordierite monolith, and one of the conclusions reported was that the calcination procedure affects the Rh-Ce-Pr interactions and the homogeneous distribution of the active phases on the substrate. It was observed that catalysts prepared by flash calcinations, consisting of introducing the monolith impregnated with metal precursor salts in a previously heated furnace, are more active for N_2O decomposition than the counterpart catalysts calcined by a conventional ramp heating. Flash calcination improved the homogeneous distribution of the active phase on the substrate and smaller rhodium particles were obtained by this procedure, improving the reduction of surface Rh-Ce-Pr entities at low temperature. However, it was not possible to analyze the effect of the calcination rate on the active phase properties due to the low mass of active phase with regard to the mass of cordierite support. The improved activity of RhOx/Ceria catalysts prepared by flash calcination was also demonstrated for the CO oxidation reaction [19]. Nevertheless, a detailed study of the effect of the calcination rate both of the ceria support and of the rhodium nitrate, starting calcination at different temperatures, has never been reported for N_2O decomposition RhOx/ceria catalysts.

The goal of this study is to get further insights into the effect of the calcination conditions on the metal-support interaction and catalytic activity for N_2O decomposition of $RhOx/CeO_2$ catalysts. For this purpose, powder catalysts have been prepared following different ramp and flash calcination conditions, analyzing the effect on the physico-chemical properties and catalytic activity for N_2O decomposition of the resulting model $RhOx/CeO_2$ catalysts.

2. Experimental Section

2.1. Catalyst Preparation

Four RhOx/CeO_2 catalysts were prepared, referred to as Rh25Ce25, Rh250Ce25, Rh350Ce25 and Rh350Ce250. The number after each metal symbol corresponds to the starting temperature for calcinations. Powder CeO_2 was prepared by $Ce(NO_3)_3 \cdot 6H_2O$ (Alfa-Aesar, Karlsruhe, Baden-Wurtemberg, Germany, 99.5%) calcination in two different ways:

Ramp calcination: Consisted of heating the cerium precursor in a muffle furnace (static air) from 25 to 600 °C at 10 °C/min, maintaining the maximum temperature for 90 min. This ceria support is referred to as Ce25.

Flash calcination: Consisted of heating the muffle furnace at 250 °C. Then, the cerium precursor was introduced and the temperature was raised at 10 °C/min up to 600 °C, maintaining the maximum temperature for 90 min. This ceria support is referred to as Ce250.

Rhodium was loaded on both ceria powders by incipient wetness impregnation with an aqueous solution of $Rh(NO_3)_3 \cdot xH_2O$ (Sigma-Aldrich, Tres Cantos, Madrid, Spain, ~36 wt.% as Rh) of the appropriate concentration to obtain 2.5 wt.% of Rhodium over CeO_2. The impregnated cerias were placed in the furnace immediately after impregnation. The rhodium precursor decomposition was also performed using different calcination conditions (ramp and flash). The furnace temperature was stabilized at 25 °C (ramp calcination) or at 250 or 350 °C (flash calcinations) before the sample is introduced (denoted by Rh25, Rh250 and Rh350, respectively). In all cases, the heating rate was 10 °C/min and the final temperature was 500 °C, maintaining this temperature for 30 min.

2.2. Catalysts Characterization

Ten mg of either $Ce(NO_3)_3 \cdot 6H_2O$ or rhodium nitrate impregnated on Ce25 ($Rh(NO_3)_3$/Ce25) were decomposed in a thermobalance TG-DTA (METTLER TOLEDO model TGA/SDTA851e/LF/1600, L'Hospitalet de Llobregat, Barcelona, Spain) coupled to a mass spectrometer (PFEIFFER VACUUM model THERMOSTAR GSD301T, Alcobendas, Madrid, Spain) under 100 mL/min flow of synthetic air, with a heating rate of 50 °C/min.

A Bruker D8-advance device (Rivas Vaciamadrid, Madrid, Spain) was used to obtain diffractograms between 10° and 80° (2θ), with steps of 0.02° and a step time of 3 s. CuKα radiation (λ = 1.540598 Å) was used. The average crystal size (D) was determined using the Scherrer and Williamson-Hall equations [20].

Raman spectra were recorded in a Jobin Yvon Horiba Raman dispersive spectrometer with a variable-power He-Ne laser source (632.8 nm) and using a confocal microscope with a 50× objective of long focal length (Horiba Scientific, Tres Cantos, Madrid, Spain). The spectrum of each sample was obtained as the average signal of 12 individual spectra of different areas of the sample. The acquisition time for each individual spectrum was 10 s.

Physical adsorption and desorption isotherms of N_2 were obtained at −196 °C in an automatic volumetric system (Autosorb-6, Quantachrome GmbH & Co. KG, Odelzhausen, Upper Bavaria, Germany). Samples were outgassed at 150 °C for 4 h under vacuum before the N_2 adsorption measurements. The BET surface areas were determined from the N_2 adsorption isotherms.

Experiments of temperature programmed reduction with H_2 (H_2-TPR) were carried out in a Micromeritics Pulse ChemiSorb 2705 device, (Micromeritics Germany GmbH, Aachen, North Rhine-Westphalia Germany), consisting of a tubular quartz reactor (inner diameter 5 mm) coupled to a TCD analyzer. A cold trap consisting of a mixture of isopropyl alcohol and liquid nitrogen at −89 °C was placed before the TCD. 20 mg of fresh catalyst were pre-treated *in situ* at 500 °C for 1 h in a 50 mL/min flow of 5% O_2 in He. After cooling to room temperature, the flow gas was switched to 40 mL/min of 5 vol% H_2 in Ar and the temperature was increased at 10 °C/min up to 1050 °C.

TEM characterization was performed using a JEOL (JEM-2010) microscope, equipped with an EDS analyzer (OXFORD, model INCA Energy TEM100, Wiesbaden, Hesse, Germany). The samples were dispersed on ethanol and placed on a cupper grid with lacey carbon film. The Rh particle size distribution was estimated on a selected catalyst from the TEM pictures. For this estimation, the size of around 100 rhodium particles was measured with the software analiSYS.

XPS characterization of selected catalysts was carried out in a VG-Microtech Multilab electron spectrometer using a MgKα (1253.6 eV) radiation source. To obtain the XPS spectra, the pressure of the analysis chamber was maintained at 5×10^{-10} mbar. The binding energy (BE) and the kinetic energy (KE) scales were adjusted by setting the C1s transition at 284.6 eV, and BE and KE values were determined with the Peak-fit software of the spectrometer. XPS spectra were recorded with selected fresh catalysts and with the same catalysts pre-treated *in situ* under N_2O at 225 °C for different periods of time. The *in situ* pre-treatments were carried out in an auxiliary reaction chamber, where the sample was heated to 225 °C and the gas mixture (1000 ppm N_2O/He, 1 atm total pressure) was fed. After the pre-treatment, the sample was introduced into the XPS chamber, avoiding exposure to air. The oxidation states of rhodium and cerium have been determined with similar assignations to those reported elsewhere [21,22].

2.3. N_2O Decomposition Tests

N_2O decomposition tests were performed in a U-shaped fix-bed quartz reactor, located in a vertical furnace at atmospheric pressure, with a 100 mL/min flow (GHSV = 42,000 h^{-1}) of 1000 ppm N_2O in He, using 100 mg of powder catalyst.

The experiments consisted of point-by-point isothermal reactions from 175 °C, increasing the temperature in intervals of 25 °C, which were extended until the steady state was reached. The gas composition was analyzed by a HP 6890 gas chromatograph equipped with a TCD and two columns (Porapak Q, for N_2O, and Molecular Sieve 13X, for O_2 and N_2).

3. Results and Discussion

3.1. TG-MS Study of Metal Precursors Decomposition

$Ce(NO_3)_3 \cdot 6H_2O$ and $Rh(NO_3)_3$/Ce25 decomposition was studied by TG-MS. The results obtained are plotted in Figure 1. In both experiments, most water molecules (*m*/*z* 18) evolved below 250 °C with the corresponding weight loss. During $Ce(NO_3)_3 \cdot 6H_2O$ decomposition (Figure 1a), three well-defined *m*/*z* 18 peaks were observed assigned to coordination water release. In the $Rh(NO_3)_3$/Ce25 decomposition

experiment (Figure 1b) a broad *m*/*z* 18 band with two maxima appeared. It must be outlined the difference in the Y-axis scales due to the low $Rh(NO_3)_3$ percentage of the sample.

Cerium nitrate (Figure 1a) decomposed in a relatively narrow range of temperature (240–320 °C) with NO (*m*/*z* 30), NO_2 (*m*/*z* 46) and O_2 (*m*/*z* 32, which is not shown for clarity) release. This result lead us to select 25 and 250 °C for the preparation of the ceria supports in ramp (slow water evolution) and flash (rapid water evolution) calcination conditions, respectively.

Figure 1. Metal precursors decomposition followed by TG-MS. (**a**) $Ce(NO_3)_3 \cdot 6H_2O$ and (**b**) $Rh(NO_3)_3$/Ce25.

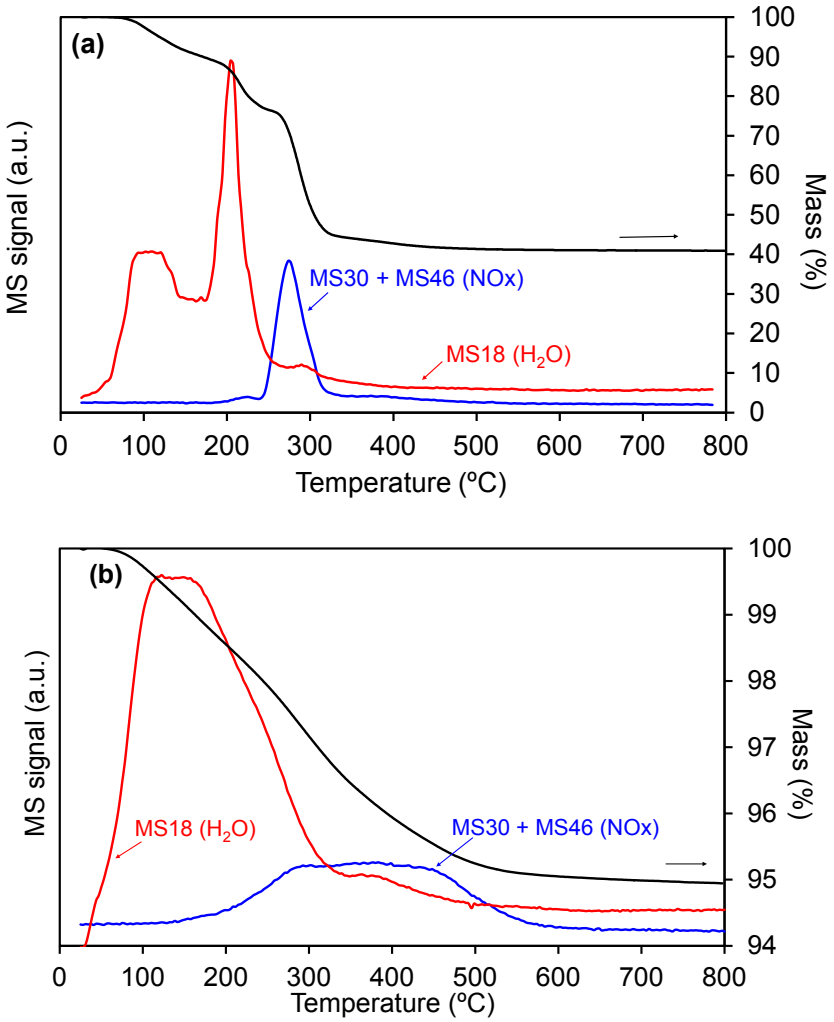

Rhodium nitrate impregnated on ceria (Figure 1b) decomposed in the range 200–550 °C, and decomposition in such wide range of temperature is an evidence of the interaction of the noble metal species (nitrate and/or oxide) with the ceria support (otherwise a narrower range of decomposition temperatures would be expected). Taking the results of Figure 1b into account, three temperatures were selected to start the calcination treatments for catalysts preparation: 25, 250 and 350 °C. In the calcination from 25 °C, water release will be slow and the impregnated rhodium salt will be allowed to move on the ceria particles surface forced by the concentration gradients created during drying. Once dry, rhodium nitrate is expected to be distributed on the ceria surface more heterogeneously than if water is released very rapidly (as in calcinations starting at 250 or 350 °C), and this heterogeneity is expected to

affect the final rhodium particle size, as it will be demonstrated afterwards. In the calcination starting at 250 °C, most of the water release will be very rapid but not the rhodium nitrate decomposition, while starting at 350 °C both water release and rhodium nitrate decomposition will be fast.

3.2. X-ray Diffraction, Raman Spectroscopy and N_2 Adsorption at −196 °C Characterization

All catalysts were characterized by XRD (Figure 2) and Raman spectroscopy (Figure 3), and both techniques provide complementary information about the structure of the ceria supports. X-ray radiation penetrates more than 1 μm into the solid giving information about the bulk structure, in particular about the cations' sublattice. On the contrary, Raman spectroscopy usually gives information of 10–100 μm deep, and in the case of cerium oxides, is useful to analyze the oxygen anions' sublattice.

Figure 2. XRD patterns of fresh catalysts.

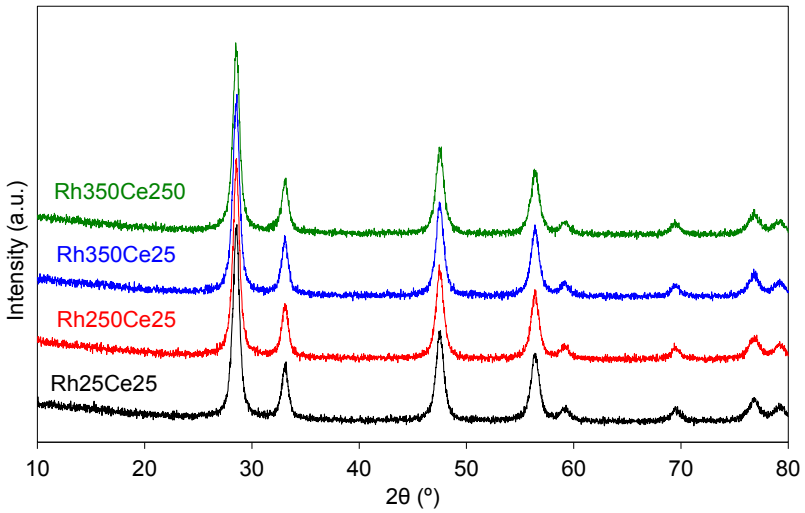

Figure 3. Raman spectra of fresh catalysts.

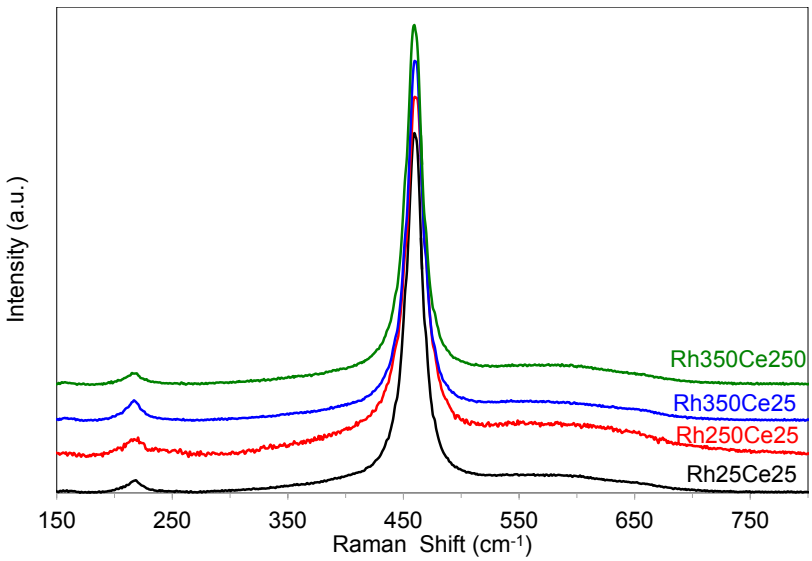

All X-Ray diffractograms (Figure 2) show fluorite structure characteristic reflections, corresponding to the planes (111), (200), (220), and (311). No other peaks but those of fluorite were observed in the

diffractograms [23] indicating that rhodium species should be highly dispersed. The average crystallite sizes of the ceria particles were determined with the Scherrer and Williamson-Hall equations. The values obtained are included in Table 1 together with the BET surface areas. Similar crystallite sizes of around 13 nm and BET surface areas of 66 ± 2 m^2/g have been found for all catalysts.

Table 1. XRD and N_2 adsorption characterization results.

Sample	Lattice Parameter (nm)	Crystal Size *by Scherrer* (nm)	Crystal Size by *Williamson-Hall* (nm)	BET Surface Area (m^2/g)
Rh25/Ce25	0.5401	12	14	64
Rh250/Ce25	0.5412	12	13	66
Rh350/Ce25	0.5401	12	13	66
Rh350/Ce250	0.5424	12	13	69

Raman spectra included in Figure 3 are also similar for all catalysts. All of them show the main band at about 460 cm^{-1} assigned to the F_{2g} mode of the fluorite-type structure of cerium oxides, based on the face-centered cubic cell [24,25], and a small peak at 230 cm^{-1} assigned to RhOx species [25–29].

In conclusion, the XRD, Raman spectroscopy and N_2 adsorption characterization reveal that all the ceria supports seems to be very similar, that is, the heating conditions used in the calcinations steps do not affect ceria properties.

3.3. Catalytic Tests

N_2O decomposition experiments were performed with a 1000 ppm N_2O/He stream and the steady-state N_2O decomposition rates and conversions obtained are plotted in Figure 4.

Figure 4. Steady-state N_2O decomposition rates and conversions as a function of temperature.

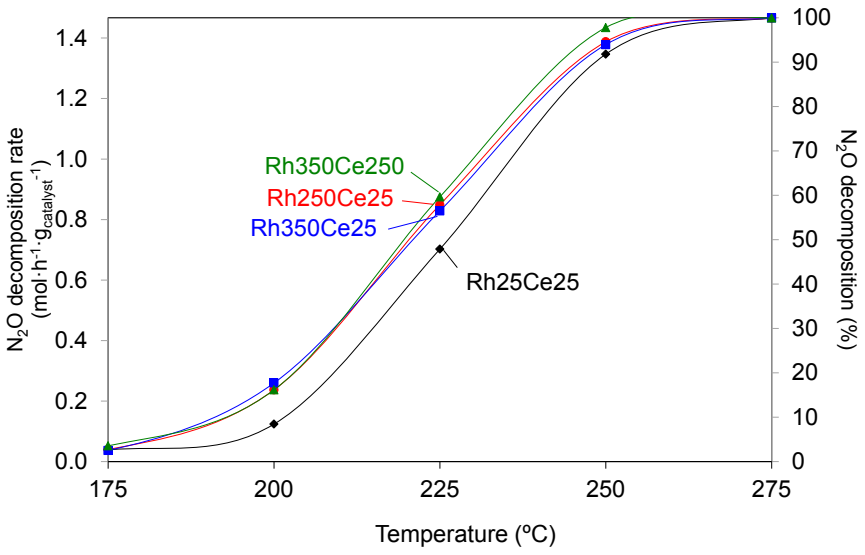

According to these results, and in agreement with previous XRD, Raman spectroscopy and N_2 adsorption characterization, the decomposition conditions of cerium nitrate has no effect on the catalytic performance (profiles for Rh350Ce25 and Rh350Ce250 are almost equal) while rhodium nitrate

decomposition affects the activity. The catalyst where rhodium nitrate was decomposed in ramp (starting heating at 25 °C (Rh25Ce25)), which is the most conventional calcination procedure, presents lower activity than catalysts calcined by a flash procedure (Rh250Ce25 and Rh350Ce25 catalysts). As postulated in a previous publication [18], this can be tentatively attributed to the improved interaction between rhodium and ceria particles obtained by flash calcinations and this interaction is studied in detail in the coming sections.

Additional information about the catalyst performance is obtained from the N_2O decomposition profiles as a function of time for the different temperatures, that is, from the behavior of the N_2O decomposition profiles before the steady-state is achieved. The steady state was reached after 20–30 min of reaction for all temperatures and catalysts, except for experiments performed at 225 °C, where longer times were required to reach a constant N_2O decomposition level. These curves are included in Figure 5 for selected catalysts (Rh25Ce25 and Rh250Ce25; rhodium decomposed by ramp and flash calcinations, respectively).

Figure 5. N_2O decomposition at 225 °C as a function of time.

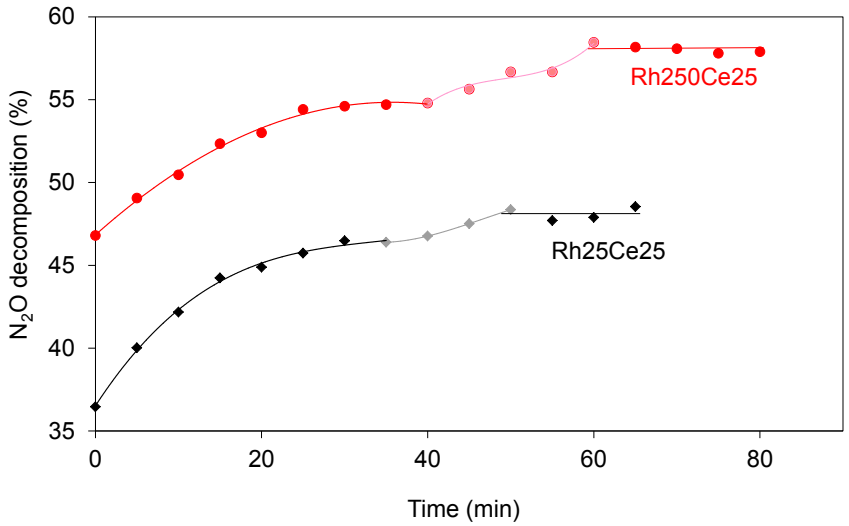

From a qualitative point of view, both profiles are similar, with a first step of 35–40 min where the N_2O decomposition level increased until a pseudo steady-state was reached. The conversions then increased again for 20–25 additional minutes before the real steady-state level was stabilized. Despite both profiles on Figure 5 being qualitatively similar, the sample Rh250Ce25 needed more time to reach the final steady-state than Rh25Ce25, the former also being more active than the latter. The transformations suffered by these two catalysts before the steady state was achieved at 225 °C were studied by XPS.

3.4. Characterization by XPS of Fresh Catalysts and after in Situ Pre-Treatments with N_2O at 225 °C

XPS spectra were recorded with the fresh Rh250Ce25 and Rh25Ce25 catalysts and with these catalysts pre-treated *in situ* with 1000 ppm N_2O/He at 225 °C for different periods of time. The profiles obtained for the Rh 3d and Ce 3d transitions were qualitatively similar to those previously obtained with some other rhodium/ceria catalysts [21,22,29]. The percentages of Rh (0) (with regard to total rhodium) and Ce (III) (with regard to total cerium) were calculated similarly to that reported elsewhere [21,22,29]. Figure 6 compiles these Rh (0) and Ce (III) percentages.

Rhodium appeared fully oxidized on both fresh catalysts (t = 0 min), which was expected since the catalysts were calcined at 500 °C, and the Ce (III) percentages (38%–40%) were in accordance with values typically obtained with these materials [21,22,29].

During the N_2O pre-treatments, the catalysts were first reduced and re-oxidised afterwards. As observed in Figure 6, rhodium was progressively reduced and only Rh (0) was identified in both catalysts after the 15 min pretreatment, while after 60 min both Rh (III) and Rh (0) were observed again. The behavior of the cerium oxidation state (Figure 6) was qualitatively similar to that of rhodium, Ce (IV) being first slightly reduced to Ce (III) and reoxidised afterwards. It has to be mentioned that only the trend of the cerium oxidation state must be considered, but not the absolute values, since the reducing environment of the XPS measurements (high vacuum and an electron beam) could affect such absolute oxidation state values.

Figure 6. (**a**) Rh (0) and (**b**) Ce (III) percentages determined by XPS after *in situ* thermal treatments with 1000 ppm N_2O at 225 °C for different times.

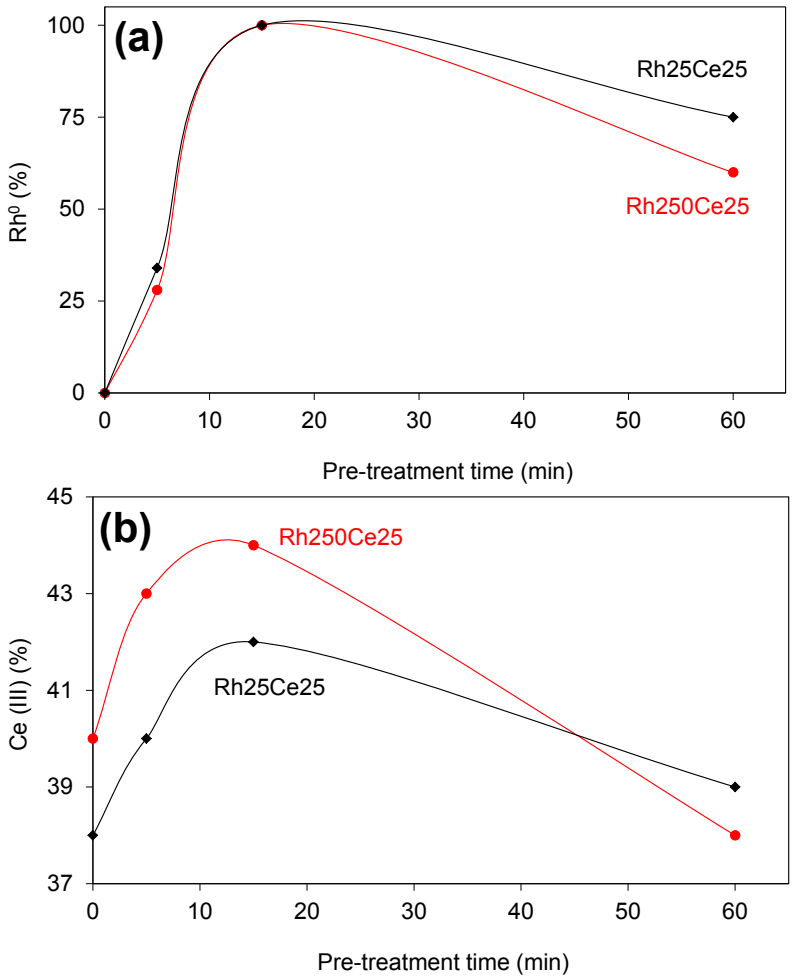

These XPS results (Figure 6), together with the N_2O conversion profiles included in Figure 5, evidence that the $RhOx/CeO_2$ catalysts suffer an activation process at 225 °C. The reduction of Rh (III) to Rh (0) after 15 min suggests that the interaction between RhOx with ceria is poor on fresh catalysts, otherwise it would be expected that rhodium remains partially oxidized due to the rhodium-ceria interaction [29]. Only after some time the real steady state is achieved, and both rhodium and cerium

appear partially reoxidised evidencing that some surface transformations have occurred. The reoxidation of the catalysts (both of rhodium and cerium) is stronger for the most active catalyst (Rh250Ce25; see Figure 6 for time =60 min), suggesting a deeper transformation during the activation period. The easier reduction of Rhodium on the ramp calcination catalyst could be related to a worst stabilizing effect of the ceria support.

3.5. H_2-TPR Characterization

Additional information about the redox properties of the catalysts was obtained by H_2-TPR. The TCD profiles obtained in H_2-TPR experiments are included in Figure 7. Three peaks are observed for all catalysts. The H_2 consumed above 700 °C is assigned to bulk ceria reduction, that is, to the reduction of Ce (IV) cations placed within the oxide particles. The lowest-temperature peak at around 100 °C is attributed to both rhodium oxide reduction and noble metal-catalyzed surface reduction of ceria [30]. The TCD signal appearing between 200 and 400 °C can be attributed to different events: the reduction of surface ceria which is not in close contact with rhodium, the decomposition of surface carbonates (occluded within the CeO_2 structure) and/or the reduction of hydroxyl and peroxide/superoxide surface groups [8,31–33].

Figure 7. H_2-TPR profiles of fresh catalysts after an *in situ* pretreatment with 5% O_2/He at 500 °C.

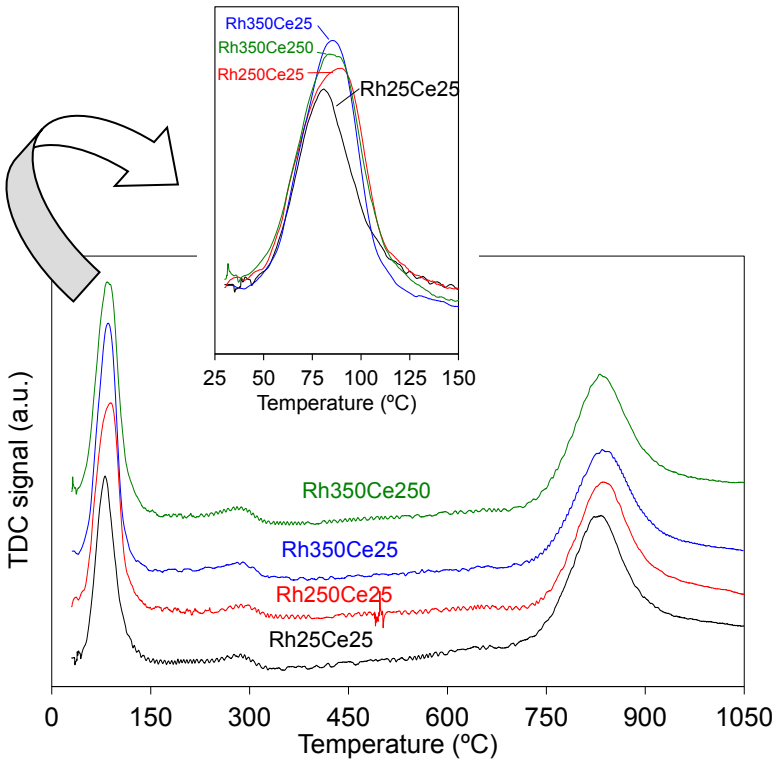

A detailed analysis of the lowest temperature reduction peak shows a slightly lower reducibility of the catalyst with the lowest activity (Rh25Ce25, see lowest area in the Figure 7) in comparison to the remaining catalysts. This observation is in agreement with the conclusions of previous studies, where a relationship between surface reducibility and N_2O decomposition capacity was obtained for a set of

$RhOx/CeO_2$ catalysts prepared with different ceria carriers (either pure and doped with La or Pr) [17]. Moreover, the rate limiting step of the $RhOx/CeO_2$ catalyzed N_2O decomposition mechanism was reported to be the reduction of the catalysts sites by N_2O. The redox properties of the support play an important role in the stabilization of cationic rhodium species under reaction conditions, and best Rh/Ceria catalysts where those with a highly reducible CeO_2 surface. The current results suggest that flash calcination of rhodium nitrate (starting heating either at 250 or 350 °C) allows obtaining a much better noble metal-support interaction than the conventional ramp calcinations (starting heating at 25 °C) [18,29], which was confirmed by TEM analysis.

3.6. TEM Characterization

Catalysts Rh25Ce25 and Rh250Ce25 were selected for TEM microscopy characterization. Figure 8 shows, as an example, a representative micrograph of each catalyst and the particle size distribution of rhodium for Rh25Ce25.

Figure 8. TEM pictures of catalysts (**a**) Rh25Ce25; (**b**) Rh250Ce25 and (**c**) particle size distribution of rhodium for Rh25Ce25.

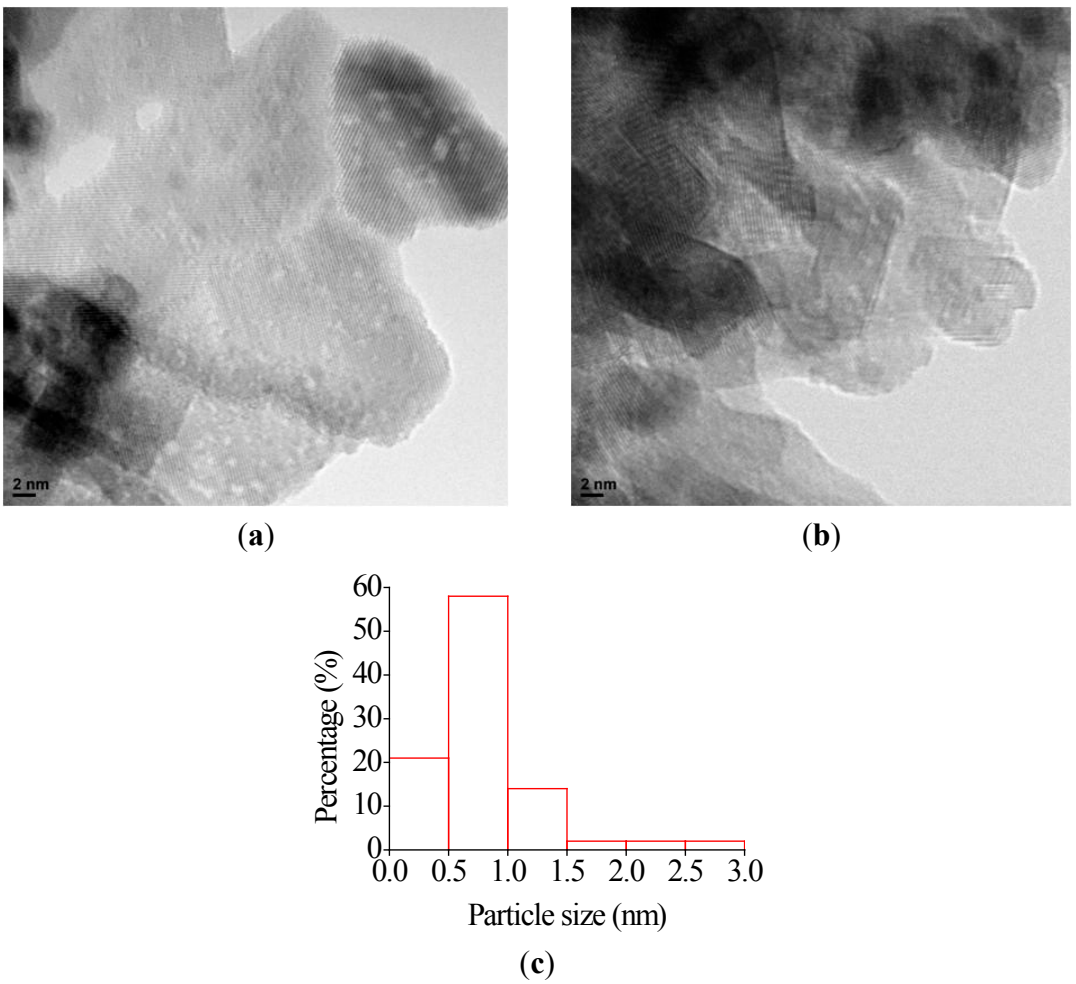

In the catalyst prepared by conventional ramp calcination (Rh25Ce25), RhOx particles smaller than 3 nm are distinguished. In this case, the number of RhOx particles which are clearly distinguished from

the ceria support is enough to make a rhodium particle size distribution. This distribution shows that most rhodium oxide nanoparticles present a size of 0.5–1 nm.

In the catalyst prepared by flash calcination of rhodium nitrate (Rh250Ce25; Figure 8b), RhOx particles have been hardly observed, assuming that most of them are much smaller than 1 nm, and evidencing a better dispersion of rhodium on this catalyst.

As a summary, smaller RhOx particles are supported on ceria by flash calcinations of impregnated rhodium nitrate in comparison to conventional ramp calcinations. Catalysts prepared by this procedure are more active than the counterpart prepared in ramp, since the RhOx-ceria interaction is improved.

4. Conclusions

The conclusions of this study can be summarized as follows:

Ramp or flash calcination of cerium nitrate to obtain the ceria support has no effect neither on the ceria properties (those observed by XRD, Raman spectroscopy and N_2 adsorption) nor on the catalyst performance for N_2O decomposition of $RhOx/CeO_2$ catalysts.

Flash calcination of rhodium nitrate impregnated on ceria improves the catalytic activity for N_2O decomposition of $RhOx/CeO_2$ catalysts in comparison to that of similar catalysts calcined in ramp.

The improved N_2O decomposition capacity of catalysts where rhodium nitrate was decomposed by flash calcinations is attributed to the smaller size of RhOx nanoparticles (which are smaller than 1 nm) allowing a better metal-support interaction.

Acknowledgments

The authors thank the financial support of Generalitat Valenciana (Project Prometeo 2009/047), the Spanish Ministry of Economy and Competitiveness (Project CTQ2012-30703), and the UE (FEDER funding).

Author Contributions

Both authors designed the experiments and wrote the paper; Verónica Rico-Pérez performed the experiments and analyzed the data.

Conflicts of Interest

The authors declare no conflict of interest.

References

1. Trovarelli, A.; de Leitenburg, C.; Boaro, M.; Dolcetti, G. The utilization of ceria in industrial catalysis. *Catal. Today* **1999**, *50*, 353–367.
2. Luo, M.F.; Ma, J.M.; Lu, J.Q.; Song, Y.P.; Wang, Y.J. High-surface area CuO-CeO_2 catalysts prepared by a surfactant-templated method for low-temperature CO oxidation. *J. Catal.* **2007**, *246*, 52–59.
3. Trovarelli, A. Catalytic Properties of Ceria and CeO_2-Containing Materials. *Catal. Rev. Sci. Eng.* **1996**, *38*, 439–520.

4. Konsolakis, M.; Drosou, C.; Yentekakis, I.V. Support mediated promotional effects of Rare Earth Oxides (CeO_2 and La_2O_3) on N_2O decomposition and N_2O reduction by CO or C_3H_6 over Pt/Al_2O_3 structured catalysts. *Appl. Catal. B* **2012**, *123*, 405–413.
5. Konsolakis, M.; Aligizou, F.; Goula, G.; Yentekakis, I.V. N_2O decomposition over doubly-promoted $Pt(K)/Al_2O_3$-(CeO_2-La_2O_3) structured catalysts: On the combined effects of promotion and feed composition. *Chem. Eng. J.* **2013**, *230*, 286–295.
6. Bernal, S.; Calvino, J.J.; Cauqui, M.A.; Gatica, J.M.; Larese, C.; Pérez Omil, J.A.; Pintado, J.M. Some recent results on metal/support interaction effects in NM/CeO_2 (NM, noble metal) catalysts. *Catal. Today* **1999**, *50*, 175–206.
7. Fornasiero, P.; Kaspar, J.; Sergo, V.; Graziani, M. Redox Behavior of High-Surface-Area Rh-, Pt-, and Pd-Loaded $Ce_{0.5}Zr_{0.5}O_2$ Mixed Oxide. *J. Catal.* **1999**, *182*, 56–69.
8. Fornasiero, P.; Dimonte, R.; Rao, G.R.; Kaspar, J.; Meriani, S.; Trovarelli, A.; Graziani, M. Rh-Loaded CeO_2-ZrO_2 Solid-Solutions as Highly Efficient Oxygen Exchangers, Dependence of the Reduction Behavior and the Oxygen Storage Capacity of the Structural-Properties. *J. Catal.* **1995**, *151*, 168–177.
9. Rao, G.; Mishra, B. Structural, redox and catalytic chemistry of ceria based materials. *Bull. Catal. Soc. India* **2003**, *2*, 122–134.
10. Ivanova, A.S. Physicochemical and Catalytic Properties of Systems Based on CeO_2. *Kinet. Catal.* **2009**, *50*, 797–815.
11. Miyazawa, T.; Okumura, K.; Kunimori, K.; Tomishige, K. Promotion of Oxidation and Reduction of Rh Species by Interaction of Rh and CeO_2 over $Rh/CeO_2/SiO_2$. *J. Phys. Chem. C* **2008**, *112*, 2574–2583.
12. Vidmar, P.; Fornasiero, P.; Kaspar, J.; Gubitosa, G.; Graziani, M. Effects of Trivalent Dopants on the Redox Properties of $Ce_{0.6}Zr_{0.4}O_2$ Mixed Oxide. *J. Catal.* **1997**, *171*, 160–168.
13. Bera, P.; Gayen, A.; Hegde, M.S.; Lalla, N.P.; Spadaro, L.; Frusteri, F.; Arena, F. Promoting Effect of CeO_2 in Combustion Synthesized Pt/CeO_2 Catalyst for CO Oxidation. *J. Phys. Chem. B* **2003**, *107*, 6122–6130.
14. He, Q.; Mukerjee, S.; Shyam, B.; Ramaker, D.; Parres-Esclapez, S.; Illán-Gómez, M.J.; Bueno-López, A. Promoting effect of CeO_2 in the electrocatalytic activity of rhodium for ethanol electro-oxidation. *J. Power Sour.* **2009**, *193*, 408–415.
15. Costa, L.O.O.; Vasconcelos, S.M.R.; Pinto, A.L.; Silva, A.M.; Mattos, L.V.; Noronha, F.B.; Borges, L.E.P. Rh/CeO_2 catalyst preparation and characterization for hydrogen production from ethanol partial oxidation. *J. Mater. Sci.* **2008**, *43*, 440–449.
16. Kaspar, J.; Fornasiero, P.; Graziani, M. Use of CeO_2-based oxides in the three-way catalysis. *Catal. Today* **1999**, *50*, 285–298.
17. Parres-Esclapez, S.; Illán-Gómez, M.J.; Salinas-Martinez de Lecea, C.; Bueno-López, A. On the importance of the catalyst redox properties in the N_2O decomposition over alumina and ceria supported Rh, Pd and Pt. *Appl. Catal. B* **2010**, *96*, 370–378.
18. Rico-Perez, V.; Parres-Esclapez, S.; Illan-Gomez, M.J.; Salinas-Martinez de Lecea, C.; Bueno-Lopez, A. Preparation, characterisation and N_2O decomposition activity of honeycomb monolith-supported $Rh/Ce_{0.9}Pr_{0.1}O_2$ catalysts. *Appl. Catal. B* **2011**, *107*, 18–25.

19. Rico-Pérez, V.; Velasco Beltrán, M.A.; He, Q.; Wang, Q.; Salinas-Martínez de Lecea, C.; Bueno-López, A. Preparation of ceria-supported rhodium oxide sub-nanoparticles with improved catalytic activity for CO oxidation. *Catal. Commun.* **2013**, *33*, 47–50.
20. Bueno-Ferrer, C.; Parres-Esclapez, S.; Lozano-Castelló, D.; Bueno-López, A. Relationship between surface area and crystal size of pure and doped cerium oxides. *J. Rare Earths* **2010**, *28*, 647–653.
21. Parres-Esclapez, S.; Such-Basañez, I.; Illán-Gómez, M.J.; Salinas-Martínez de Lecea, C.; Bueno-López, A. Study by isotopic gases and *in situ* spectroscopies (DRIFTS, XPS and Raman) of the N_2O decomposition mechanism on Rh/CeO_2 and Rh/χ-Al_2O_3 catalysts. *J. Catal.* **2010**, *276*, 390–401.
22. Guillén-Hurtado, N.; Atribak, I.; Bueno-López, A.; García-García, A. Influence of the cerium precursor on the physico-chemical features and NO to NO_2 oxidation activity of ceria and ceria-zirconia catalysts. *J. Mol. Catal. A Chem.* **2010**, *323*, 52–58.
23. Terribile, D.; Trovarelli, A.; Llorca, J.; de Leitenburg, C.; Dolcetti, G. The preparation of high surface area CeO_2-ZrO_2 mixed oxides by a surfactant-assisted approach. *Catal. Today* **1998**, *43*, 79–88.
24. Mineshige, A.; Taji, T.; Muroi, Y.; Kobune, M.; Fujii, S.; Nishi, N.; Inaba, M.; Ogumi, Z. Oxygen chemical potential variation in ceria-based solid oxide fuel cells determined by Raman spectroscopy. *Solid State Ionics* **2000**, *135*, 481–485.
25. Bueno-Lopez, A.; Krishna, K.; Makkee, M.; Moulijn, J.A. Enhanced soot oxidation by lattice oxygen via La^{3+}-doped CeO_2. *J. Catal.* **2005**, *230*, 237–248.
26. Music, S.; Saric, A.; Popovic, S.; Ivanda, M. Formation and characterisation of nanosize α-Rh_2O_3 particles. *J. Mol. Struct.* **2009**, *924*, 221–224.
27. Pushkarev, V.V.; Kovalchuk, V.I.; d'Itri, J.L. Probing Defect Sites on the CeO_2 Surface with Dioxygen. *J. Phys. Chem. B* **2004**, *108*, 5341–5348.
28. Nakajima, A.; Yoshihara, A.; Ishigame, M. Defect-induced Raman spectra in doped CeO_2. *Phys. Rev. B* **1994**, *50*, 13297–13307.
29. Bueno-López, A.; Such-Basáñez, I.; Salinas-Martínez de Lecea, C. Stabilization of active Rh_2O_3 species for catalytic decomposition of N_2O on La-, Pr-doped CeO_2. *J. Catal.* **2006**, *244*, 102–112.
30. Silvestre-Albero, J.; Rodríguez-Reinoso, F.; Sepúlveda-Escribano, A. Improved Metal-Support Interaction in Pt/CeO_2-SiO_2 Catalysts after Zinc Addition. *J. Catal.* **2002**, *210*, 127–136.
31. Zotin, F.M.Z.; Tournayan, L.; Varloud, J.; Perrichon, V.; Frety, R. Temperature-programmed reduction, limitation of the technique for determining the extent of reduction of either pure ceria or ceria modified by additives. *Appl. Catal. A* **1993**, *98*, 99–114.
32. Trovarelli, A. *Catalysis by Ceria and Related Materials*; Catalytic Science Series; Imperial College Press: London, UK, 2002; Volume 2, pp. 51–83.
33. Bernal, S.; Calvino, J.J.; Cifredo, G.A.; Gatica, J.M.; Perez Omil, J.A.; Pintado, J.M. Hydrogen Chemisorption on Ceria, Influence of the Oxide Surface Area and Degree of Reduction. *J. Chem. Soc. Faraday Trans.* **1993**, *89*, 3499–3505.